Convergence Analyses of 1-Node and 2-Node CMFD Schemes for the Neutron Transport

HyeonTae Kim and Yonghee Kim*

*Department of Nuclear & Quantum Engineering, Korea Advanced Institute of Science and Technology (KAIST),
Daejeon 34141, Republic of Korea*
Corresponding author: yongheekim@kaist.ac.kr

1. Introduction

Ever since nonlinear coarse mesh finite difference (CMFD) method had been introduced by K. Smith in 1983 [1], the method has been successfully implemented for accelerating the process of solving both neutron diffusion and transport equations. However, stability issues on the method were observed in some practical applications. In order to understand these phenomena, Fourier analysis was applied for CMFD and its modified versions [2].

One of those variants, one-node CMFD, proposed by Shin, et. al. in 1999 [3], handles local fine mesh analysis individually, therefore, suitable for parallel computing environments. In this paper, convergence of CMFD with one-node kernel is investigated with both analytic and numerical approach, and compare that of two-node kernel CMFD. Also, we suggest application of partial current based CMFD acceleration (p-CMFD) in one-node basis as a way of convergence enhancement for both sequential and parallel computing environments.

2. Discrete One-node CMFD

The following one dimensional reactor model is divided into coarse meshes indexed as i, and they are subdivided into p number of equally sized fine meshes.
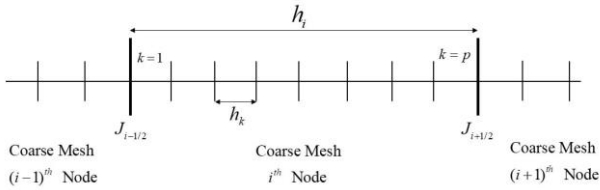
Fig. 1. One dimensional coarse/fine mesh divisions.

For the right side boundary of ith coarse mesh, currents at $\pm$ infinitesimal distance from the boundary are expressed as follows with corresponding correction factors, $\hat{D}_{i+1/2}^{-\varepsilon}$ and $\hat{D}_{i+1/2}^{+\varepsilon}$.

$$J_{i+1/2}^{-\varepsilon} = -\frac{2D_i}{h_i}\left(\phi_{i+1/2} - \overline{\phi}_i\right) - \frac{2\hat{D}_{i+1/2}^{-\varepsilon}}{h_i}\left(\phi_{i+1/2} + \overline{\phi}_i\right) \quad (1)$$

$$J_{i+1/2}^{+\varepsilon} = -\frac{2D_{i+1}}{h_{i+1}}\left(\overline{\phi}_{i+1} - \phi_{i+1/2}\right) + \frac{2\hat{D}_{i+1/2}^{+\varepsilon}}{h_{i+1}}\left(\overline{\phi}_{i+1} + \phi_{i+1/2}\right) \quad (2)$$

Equating Eq. (1) and (2) in order to meet neutron current continuity will give:

$$\phi_{i+1/2} = \frac{\left(D_i - \hat{D}_{i+1/2}^{-\varepsilon}\right)\overline{\phi} + \left(D_{i+1} - \hat{D}_{i+1/2}^{+\varepsilon}\right)\overline{\phi}_{i+1}}{D_i + D_{i+1} + \hat{D}_{i+1/2}^{-\varepsilon} + \hat{D}_{i+1/2}^{+\varepsilon}} \quad (3)$$

$$J_{i+1/2} = -\frac{2\left(D_i D_{i+1} - \hat{D}_{i+1/2}^{-\varepsilon}\hat{D}_{i+1/2}^{+\varepsilon}\right)}{D_i + D_{i+1} + \hat{D}_{i+1/2}^{-\varepsilon} + \hat{D}_{i+1/2}^{+\varepsilon}}\frac{1}{hp}\left(\overline{\phi}_{i+1} - \overline{\phi}_i\right)$$
$$-\frac{2\left(\hat{D}_{i+1/2}^{-\varepsilon}D_{i+1} - D_i\hat{D}_{i+1/2}^{+\varepsilon}\right)}{D_i + D_{i+1} + \hat{D}_{i+1/2}^{-\varepsilon} + \hat{D}_{i+1/2}^{+\varepsilon}}\frac{1}{hp}\left(\overline{\phi}_{i+1} + \overline{\phi}_i\right) \quad (4)$$

Also from (1) and (2),

$$\hat{D}_{i+1/2}^{-\varepsilon} = -\frac{J_{i+1/2}^{l+1/2}h_i + 2D_i\left(\phi_{i+1/2}^{l+1/2} - \overline{\phi}_i^{l+1/2}\right)}{2\left(\phi_{i+1/2}^{l+1/2} + \overline{\phi}_i^{l+1/2}\right)}, \quad (5)$$

$$\hat{D}_{i+1/2}^{+\varepsilon} = \frac{J_{i+1/2}^{l+1/2}h_{i+1} + 2D_{i+1}\left(\overline{\phi}_{i+1}^{l+1/2} - \phi_{i+1/2}^{l+1/2}\right)}{2\left(\phi_{i+1/2}^{l+1/2} + \overline{\phi}_{i+1}^{l+1/2}\right)}, \quad (6)$$

and the correction factors are updated from local fine mesh calculation.

2.1 Coarse mesh equations

Continuity equation for i^{th} coarse mesh:

$$J_{i+1/2}^{l+1} - J_{i-1/2}^{l+1} + \sum_k h_k \sigma_{r,ki}\phi_{ki}^{l+1} = \sum_k h_k q_k \quad (7)$$

Here, surface net current is approximated as:

$$J_{i+1/2}^{l+1/2} = \frac{1}{2}\sum_{n=1}^{N} w_n \mu_n \psi_{n,i+1/2}^{l+1/2} \quad (8)$$

where

$$\phi_i^{l+1/2} = \frac{1}{2}\sum_{n=1}^{N} w_n \psi_{n,i}^{l+1/2}$$

$(\mu_n, w_n) =$ discrete ordinate quadrature set.

2.2 Fine mesh equations

In the slab geometry, neutron transport equation in fine mesh is expressed as follows:

$$\mu\frac{d}{dx}\psi^{l+1/2}(x,\mu) + \sigma_t(x)\psi^{l+1/2}(x,\mu) = \sigma_s(x)\phi^l(x) + q(x). \quad (9)$$

Discretizing the transport equation with diamond-differencing and quadrature set will give:

$$\mu_n \frac{\psi_{n,k+1/2}^{l+1/2} - \psi_{n,k-1/2}^{l+1/2}}{h} + \sigma_t \frac{\psi_{n,k+1/2}^{l+1/2} + \psi_{n,k-1/2}^{l+1/2}}{2} = \sigma_s \phi_k^l + Q, \quad (10)$$

$$\phi_k^{l+1/2} = \frac{1}{2} \sum_{n=1}^{N} w_n \frac{\psi_{n,k+1/2}^{l+1/2} + \psi_{n,k-1/2}^{l+1/2}}{2}. \quad (11)$$

3. Fourier Analysis of One-node CMFD

In this paper, analytic approach is made with uniform mesh size, constant properties, and flat source reactor with all-reflective boundaries. For the given condition, scalar flux is Q/σ_r.

Now, we introduce input for initial iteration step:

$$\bar{\phi}_i^{l+1} = \frac{Q}{\sigma_r} \left(1 + \varepsilon \zeta_i^{l+1} \right), \quad (12a)$$

$$\bar{\phi}_i^{l+1/2} = \frac{Q}{\sigma_r} \left(1 + \varepsilon \zeta_i^{l+1/2} \right), \quad (12b)$$

$$\psi_{n,i+1/2}^{l+1/2} = \frac{Q}{\sigma_r} \left(1 + \varepsilon \xi_{i+1/2}^{l+1/2} \right). \quad (12c)$$

to both coarse and fine mesh equations. Then choose $O(\varepsilon)$ terms only to linearize for error ε, while $O(1)$ shows trivial result.

From local fine mesh equations, we get:

$$\mu_n \frac{\xi_{n,k+1/2}^{l+1/2} - \xi_{n,k-1/2}^{l+1/2}}{h} + \sigma_t \frac{\xi_{n,k+1/2}^{l+1/2} + \xi_{n,k-1/2}^{l+1/2}}{2} = \sigma_s \zeta_k^l \quad (13)$$

$$\zeta_k^{l+1/2} = \frac{1}{2} \sum_{n=1}^{N} w_n \frac{\xi_{n,k+1/2}^{l+1/2} + \xi_{n,k-1/2}^{l+1/2}}{2} \quad (14)$$

Also from Eq. (13) and (14), relation between $\xi_{n,i\pm1/2}^{l+1/2}$, ζ_k^l, and ζ_k^{l+1} is obtained:

$$\frac{1}{2} \sum_n w_n \mu_n \left(\xi_{n,i+1/2}^{l+1/2} - \xi_{n,i-1/2}^{l+1/2} \right)$$
$$= -h\sigma_t \sum_k \zeta_k^{l+1/2} + h\sigma_s \sum_k \zeta_k^l \quad (15)$$

After some algebra, global coarse mesh equation (7) and (8) will be:

$$\left[D\zeta_{i-1}^{l+1/2} - 2D\zeta_i^{l+1/2} + D\zeta_{i+1}^{l+1/2} \right]$$
$$+ hp \left[\frac{1}{2} \sum_n w_n \mu_n \xi_{n,i+1/2}^{l+1/2} - \frac{1}{2} \sum_n w_n \mu_n \xi_{n,i-1/2}^{l+1/2} \right]$$
$$= \left[D\zeta_{i-1}^{l+1} + \left(-2D - h^2 p^2 \sigma_r \right) \zeta_i^{l+1} + D\zeta_{i+1}^{l+1} \right] \quad (16)$$

Applying Eq. (15) to Eq. (16) and using $D = 1/3\sigma_t$ give the final form of linearized iteration:

$$\frac{1}{3hp\sigma_t} \zeta_{i-1}^{l+1/2} - \frac{2}{3hp\sigma_t} \zeta_i^{l+1/2} + \frac{1}{3hp\sigma_t} \zeta_{i+1}^{l+1/2}$$
$$- h\sigma_t \sum_k \zeta_k^{l+1/2} + h\sigma_s \sum_k \zeta_k^l$$
$$= \frac{1}{3hp\sigma_t} \zeta_{i-1}^{l+1} + \left(-\frac{2}{3hp\sigma_t} - hp\sigma_r \right) \zeta_i^{l+1} + \frac{1}{3hp\sigma_t} \zeta_{i+1}^{l+1} \quad (17)$$

And from flux modulation,

$$\zeta_k^{l+1} = \zeta_k^{l+1/2} + \zeta_i^{l+1} - \frac{1}{p} \sum_k \zeta_k^{l+1/2} \quad (18)$$

For the case of uniform mesh and infinite medium, choice of the following Fourier ansatz is appropriate:

$$\zeta_i^l = \omega^l A \exp\left(j\lambda x_i \right), \quad (19a)$$

$$\zeta_k^l = \omega^l A_k \exp\left(j\lambda x_k \right), \quad (19b)$$

$$\zeta_i^{l+1/2} = \omega^l B \exp\left(j\lambda x_i \right), \quad (19c)$$

$$\zeta_k^{l+1/2} = \omega^l B_k \exp\left(j\lambda x_k \right), \quad (19d)$$

$$\xi_{k+1/2}^{l+1/2} = \omega^l a_{n,k} \exp\left(j\lambda x_{k+1/2} \right). \quad (19e)$$

Introducing Eq. (19) to Eqs. (17) and (18) and solving the resulted eigenvalue problem numerically lead us to plot the following spectral radius curves for different scattering ratios.
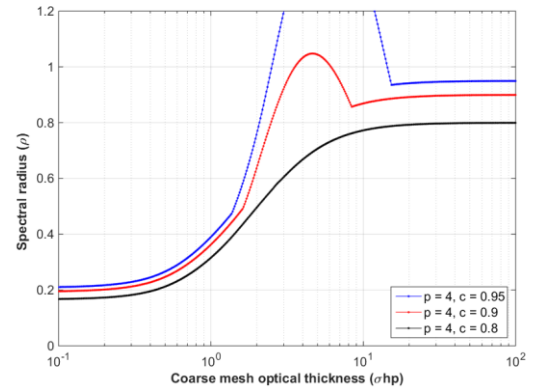
Fig. 2. Spectral radius of one-node CMFD for $p = 4$.

Notice that from Eq. (17), linearized form of one-node CMFD is exactly same with that of CMFD with two-node kernel [4], as a result, the same conditional instability is observed for near-unity scattering ratio problems.

In Fig. 2, the instability begins to develop when the optical thickness is slightly above 1 and the scattering ratio is rather high, and it mainly broadens to larger optical thickness region with increasing scattering ratio. Since a larger scattering ratio results in a lower absorption, effects of neutrons from adjacent nodes will be more significant, and therefore more iterations are needed for convergence.

4. Application of p-CMFD in One-node Basis

Partial current-based coarse mesh finite difference (p-CMFD) acceleration is developed specifically to solve the divergence issues of CMFD for the cases with large optical thickness. This method preserves two partial currents at each interface with two correction factors:

$$J_{i+1/2}^+ = -\frac{\tilde{D}_i(\bar{\phi}_{i+1} - \bar{\phi}_i) + 2\hat{D}_{i+1/2}^+ \bar{\phi}_i}{2} \qquad (20)$$

$$J_{i+1/2}^- = \frac{\tilde{D}_i(\bar{\phi}_{i+1} - \bar{\phi}_i) + 2\hat{D}_{i+1/2}^- \bar{\phi}_{i+1}}{2} \qquad (21)$$

$$J_{i+1/2}^+ - J_{i+1/2}^- = J_{i+1/2}$$
$$= -\tilde{D}_i(\bar{\phi}_{i+1} - \bar{\phi}_i) - (\hat{D}_{i+1/2}^+ \bar{\phi}_i + \hat{D}_{i+1/2}^- \bar{\phi}_{i+1}) \qquad (22)$$

On the other hand, one-node CMFD also produce outgoing partial currents from incoming partial currents, so $\hat{D}_{i+1/2}^\pm$ can be updated in the same manner as it's done in two-node kernel p-CMFD acceleration. From this, CMFD and p-CMFD with one-node kernel will be compared in the following numerical studies, both for sequential and parallel computation algorithms.

5. Numerical Tests

In this chapter, one-node CMFD and p-CMFD were tested for 1-D slab homogeneous reactor with vacuum boundary condition on each side, both for sequential and parallel calculation. The problem size is 1000 cm, $\sigma = 1\,cm^{-1}$, and flat fixed source of $Q = 1.0\ \#/cm^3\sec$. The convergences are measured in terms of numerical spectral radius defined as,

$$\rho_{num} = \frac{\|\phi^{(l)} - \phi^{(l-1)}\|_2}{\|\phi^{(l-1)} - \phi^{(l-2)}\|_2}, \qquad (23)$$

and plotted with corresponding optical thickness. The S$_{16}$ Gauss-Legendre quadrature set was used in the following evaluations.

5.1 Sequential calculations

Sequential calculation of CMFD and p-CMFD in one-node basis show similar behavior with that of Fourier analysis results. Since Fourier analysis doesn't consider boundary condition updates and kernel-wise analysis, it is equivalent to sequential calculation process.

From scattering ratio of 0.9, unstable region is expected from Fourier analysis, and observed from numerical result as well for the case of CMFD with one-node kernel. However, acceleration of p-CMFD formulation solves the instability issue as Fourier analysis result shows.
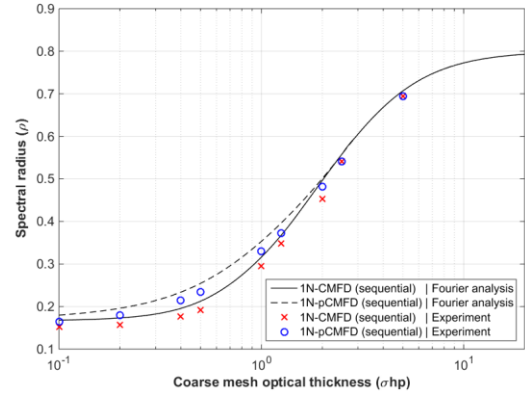
Fig. 3. Sequential calculation of 1N-CMFD and 1N-pCMFD and comparison with Fourier analysis for the case of $c = 0.8$.
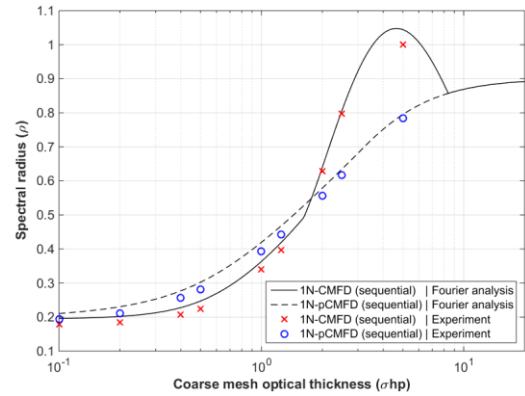
Fig. 4. Sequential calculation of 1N-CMFD and 1N-pCMFD and comparison with Fourier analysis for the case of $c = 0.9$.

5.2 Parallel calculations

For parallel calculation, there are several options regarding each local problem's boundary conditions:

i) we can use previous local angular flux,

$$\Psi_{\pm n,g}^{new,local} = \psi_{\pm n,g}^{local} \qquad (24)$$

ii) or modulate using ratio of incoming partial currents,

$$\Psi_{\pm n,g}^{new,local} = \psi_{\pm n,g}^{local} \frac{J_g^{\pm,global}}{J_g^{\pm,local}}. \qquad (25)$$

Alternative update options would include flux scaling and P$_1$-like distribution shape assumption. However, boundary angular flux modulation with partial currents ratio was only considered in this paper for brevity.

Numerical result of parallel calculation algorithm with boundary condition update was different from that of sequential calculation in terms of convergence speed and behavior.
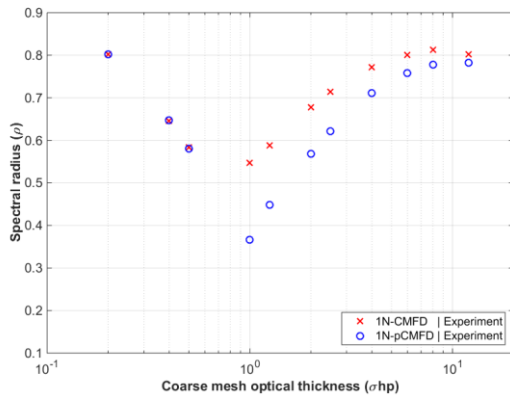
Fig. 5. Parallel calculation of 1N-CMFD and
1N-pCMFD for the case of $c = 0.8$.

By comparing figure 3 and 5, we can clearly notice that parallel calculation algorithms are showing slower convergence than sequential case. This is because of different boundary condition update strategy of them; sequential calculation updates local boundary condition for the next coarse mesh after each local analysis, while parallel algorithm updates boundary conditions for all coarse meshes at the same time, which means acceleration from the update is less effective than sequential calculation.
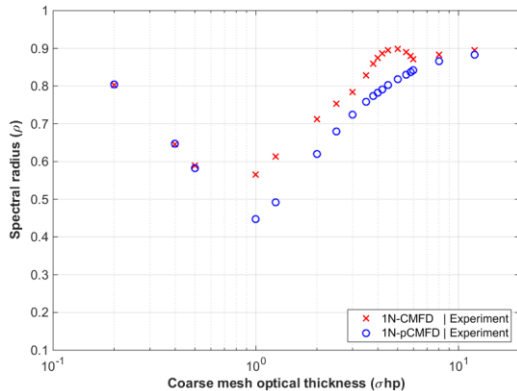
Fig. 6. Parallel calculation of 1N-CMFD and
1N-pCMFD for the case of $c = 0.9$.

From this one-node parallel calculation results, p-CMFD shows faster convergence compare to one-node CMFD in the entire section which coarse mesh optical thickness is larger than one mean free path, while potential instability spectral radius hump is observed in one-node CMFD. When coarse mesh optical thickness is smaller than one mean free path, parallel calculation schemes shows decrease of convergence as demonstrated by Kelley in his study on spatial domain-decomposed CMFD in 2012 [5].

From the numerical results, overall performance shows that p-CMFD can be considered as a better option than CMFD in one-node based parallel calculations, for practical coarse mesh optical thickness region.

6. Conclusions

In this paper, we have analyzed convergence behavior of both 1-node CMFD and 1-node p-CMFD for both sequential and parallel algorithms. For sequential calculation, the 1-node CMFD method turns out to be equivalent to the conventional 2-node CMFD in view of the convergence characteristics. In the case parallel implementation, we showed that a better convergence can be obtained with the partial current-based 1-node p-CMFD scheme than the conventional 1-node CMFD method preserving both net current and surface flux.

Theoretical analysis for parallel 1-node CMFD schemes will be performed for a better understanding of the convergence behaviors in the future.

REFERENCES

[1] K. S. Smith, "Nodal Method Storage Reduction by Non-linear Iteration," Trans. Am. Nucl. Soc., **44**, 265 (1983).
[2] N.Z. CHO and C.J. PARK, "A Comparison of Coarse Mesh Rebalance and Coarse Mesh Finite Difference Accelerations for the Neutron Transport Calculations," Proc. M&C 2003, Gatlinburg, Tennessee, USA, April 6-11,2003, American Nuclear Society (2003); see also NURAPT-2002-02, (with addendum on p-CMFD);
http://nurapt.kaist.ac.kr/lab/report/NurapT2002_2rev2.pdf.
[3] H. C. Shin, Y. H. Kim, and Y. B. Kim, "One-Node Coarse-Mesh Finite Difference Algorithm for Fine-Mesh Finite Difference Operator," Trans. Am. Nucl. Soc., **81**, 150 (1999).
[4] Akio Yamamoto, "Generalized Coarse-Mesh Rebalance Method for Acceleration of Neutron Transport Calculations", Nucl. Sci. Eng., 151, 274-282 (2005).
[5] B. W. Kelley and E. W. Larsen, "CMFD acceleration of spatial domain-decomposed neutron transport problems", PHYSOR, Knoxville, TN, USA (2012)